CHEMISTRY
A EUROPEAN JOURNAL

DOI: 10.1002/chem.200800052

The Phenoxy/Phenol/Copper Cation: A Minimalistic Model of Bonding Relations in Active Centers of Mononuclear Copper Enzymes

Petr Milko,[a] Jana Roithová,*[a, b] Detlef Schröder,[a] Joël Lemaire,[c] Helmut Schwarz,[d] and Max C. Holthausen*[e]

Dedicated to Professor Sason Shaik on the occasion of his 60th birthday

Abstract: The "bare" complex $[Cu(PhOH)(PhO)]^+$ with a phenol (PhOH) and a phenoxy (PhO) ligand bound to copper is studied both experimentally and computationally. The binding energies and structure of this complex are probed by mass spectrometry, infrared multi-photon dissociation, and DFT calculations. Further, the monoligated complexes $[Cu(PhO)]^+$ and $[Cu(PhOH)]^+$ are investigated for comparison. DFT calculations on the $[Cu(PhOH)(PhO)]^+$ complex predict that a phenolate anion interacts with copper(II) preferentially through the oxygen atom, and the bonding is associated with electron transfer to the metal center resulting in location of the unpaired electron at the aromatic moiety. Neutral phenol, on the other hand, interacts with copper preferentially through the aromatic ring. The same arrangements are also found in the monoligated complexes $[Cu(PhO)]^+$ and $[Cu(PhOH)]^+$. The calculations further indicate that the bond strength between the copper atom and the oxygen atom of the phenoxy radical is weakened by the presence of neutral phenol from 2.6 eV in bare $[Cu(PhO)]^+$ to 2.1 eV in $[Cu(PhOH)(PhO)]^+$.

Keywords: copper · density functional calculations · enzymes · IR spectroscopy · mass spectrometry · phenols

Introduction

Copper enzymes play an essential role in electron-transfer processes during photosynthesis and respiration, in the metabolism of dioxygen, in the deactivation of toxic intermediates of O_2 reduction, and within the biological nitrogen cycle, in which they mediate the reduction of nitrite or nitrous oxide.[1–5] For several decades, the nature of copper-containing active sites has been intensively studied by many research groups because of the unusual coordination geometries of copper ions, their outstanding redox potentials, absorption spectra, and electron paramagnetic resonance features, as well as their interactive role with other metal ions. Progress in metalloprotein biochemistry has profited a great deal from bioinorganic research: for nearly three decades now, a considerable body of knowledge has been accumulated from studies on the properties of small synthetic copper complexes that serve as model systems designed to mimic particular structural and/or functional aspects of their biological paragons.[2,6] For such systems it is possible to apply the whole repertoire of modern synthetic, spectroscopic, and theoretical methods to gain much more detailed insight than would be possible for biological macromolecules.

[a] Ing. P. Milko, Dr. J. Roithová, Dr. D. Schröder
Institute of Organic Chemistry and Biochemistry
Flemingovo nám. 2, 16610 Prague 6 (Czech Republic)
E-mail: roithova@natur.cuni.cz

[b] Dr. J. Roithová
Charles University in Prague
Faculty of Science, Department of Organic Chemistry
Hlavova 8, 12840 Praha 2 (Czech Republic)
Fax: (+420) 221-951-326

[c] Dr. J. Lemaire
Laboratoire Chimie-Physique, UMR8000, Université Paris-Sud
CNRS, Faculté des Sciences
Bât. 350, 91405 Orsay Cedex (France)

[d] Prof. Dr. Dr. H. Schwarz
Institut für Chemie, Technische Universität Berlin
Strasse des 17 Juni 135, 10623 Berlin (Germany)

[e] Prof. Dr. M. C. Holthausen
Institut für Anorganische und Analytische Chemie
Johann Wolfgang Goethe-Universität Frankfurt
Max-von-Laue-Strasse 7, 60438 Frankfurt am Main (Germany)
Fax: (+49) 69-798-29260
E-mail: max.holthausen@chemie.uni-frankfurt.de

Supporting information for this article is available on the WWW under http://www.chemeurj.org/ or from the author.

In metalloproteins, copper ions primarily occur in the two oxidation states +1 and +2, which are easily accessible under biological conditions. Contrary to earlier assumptions, recent bioinorganic evidence suggests that Cu^{III} might also be relevant as constituent of active sites, but so far this remains to be verified for biological systems.[7,8] Copper ions in active sites of enzymes have historically been divided into three classes according to the spectroscopic features that arise from their particular electronic structure:[9] enzymes of type 1 and type 2 contain a single copper ion, whereas type 3 sites contain dinuclear copper centers. This classification does not, however, correlate the various functions of copper proteins with the nuclearity of active sites, and both mono- and binuclear (as well as multinuclear) copper sites are involved in the diverse arrays of copper–enzyme functions. It is in fact a rather intimate interplay between the ligand environment and the redox properties associated with the coordinated copper ions that determines the intrinsic reactivity of a metal site. The nature of this fundamental structure/activity relationship is not yet fully understood, despite the enormous progress that has been made in recent years.[10–17]

The electronic interplay between ligands and a single copper ion is illustrated in the presumed catalytic cycle of the enzyme galactose oxidase (GO, Scheme 1).[18] GO is a member of the radical copper oxidase family of enzymes and contains two tyrosine moieties and a single copper ion in the active center. It is a highly efficient catalyst for the two-electron oxidation of primary alcohols to aldehydes according to $RCH_2OH \rightarrow RCHO + 2e^- + 2H^+$ directly using O_2 from air, with $O_2 + 2e^- + 2H^+ \rightarrow H_2O_2$ as the reductive half-reaction. While copper shuttles between the two oxidation states I and II, the phenoxy/phenolate groups of the tyrosine groups participate in the overall reaction as redox-active ligands, thereby enabling a two-electron redox process during the catalytic cycle.[19] Several model systems for GO have been devised, but the high catalytic efficiency of the enzyme is still far out of reach.[20–22]

Evidently a deeper understanding of the interplay between copper ions and redox-active phenol-based ligands is important, not only because this interaction is essential for the catalytic activity of enzymes like GO or glyoxal oxidase (GLO),[23] but also because it is highly relevant for technical processes.[24] Here we present a study of the structural features and the unimolecular reactivity of the simple model system Cu^{II}/phenol/phenoxy/phenolate (Scheme 2), which is examined in the gas phase by means of mass spectrometry, including infrared spectroscopy of the mass-selected cation, and quantum chemical methods.

Experimental and Computational Methods

The mass spectrometric studies were performed with three different instruments. Collision-induced dissociation (CID) mass spectra were recorded with a VG BIO-Q mass spectrometer equipped with an ESI source and of QHQ configuration (Q stands for quadrupole and H

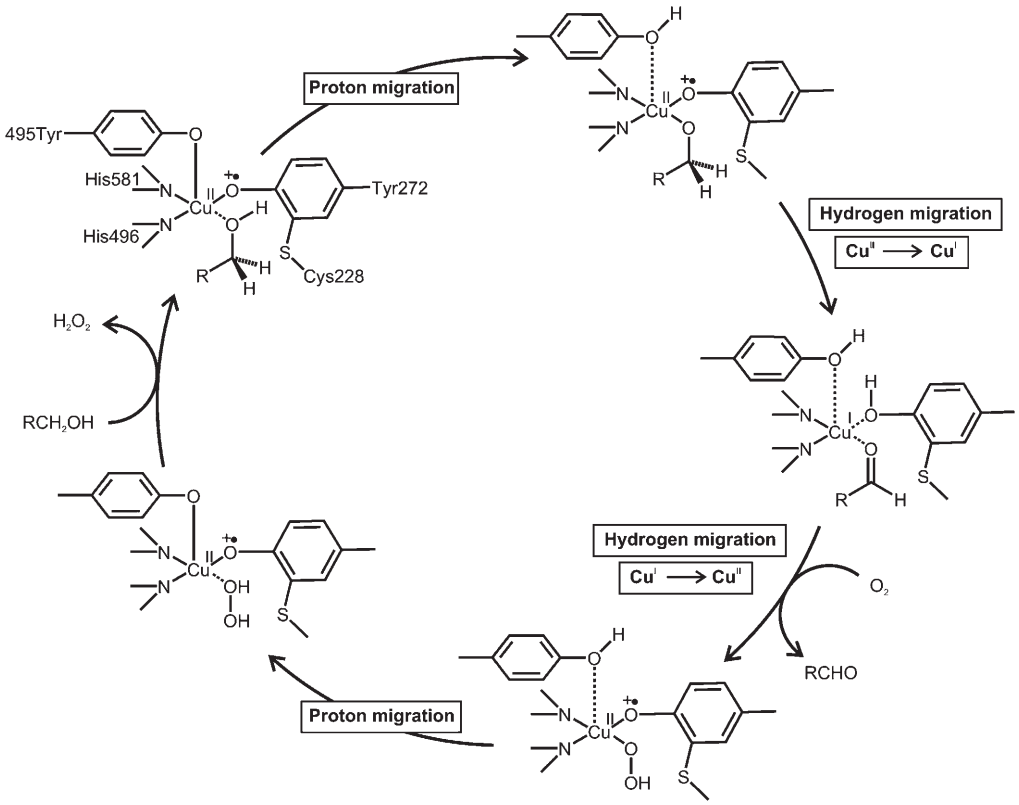

Scheme 1. Sketch of the mechanism suggested for the oxidation of alcohols in the active center of galactose oxidase.[2]

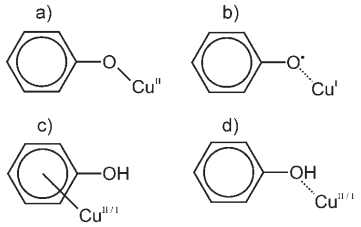

Scheme 2. Structural sketches of a) a phenolato ligand in $[Cu(PhO)]^+$, b) the alternative redox electromer of a phenoxy radical bound to Cu^I, c) a phenol ligand in a π-bound complex $[Cu(PhOH)]^{+/2+}$, and d) a phenol ligand in an O-bound complex.

stands for hexapole).[25] Three different copper salts ($Cu(NO_3)_2$, $CuCl_2$, and $CuBr_2$) dissolved in water were employed and phenol was added. The solutions were admitted to the ESI source (5 μl min^{-1}) and sprayed to the mass spectrometer with a potential of approximately 4 kV. CID experiments were performed with Q1-selected ions using xenon as collision gas in the hexapole at various collision energies (E_{lab} = 0–20 eV) and a pressure of about 2.5×10^{-4} mbar, which approximately corresponds to single collision conditions.[25] The product ions formed in the hexapole were then analyzed by scanning Q2. The collision energies were converted to the center-of-mass frame, $E_{CM}=[m/(M+m)]E_{lab}$, in which m and M are the masses of the collision gas and the ionic species, respectively. Variation of the collision energy leads to breakdown diagrams that enable the determination of phenomenological appearance energies (AEs)[26] of the various fragmentation channels by linear extrapolation of the signal onsets to the baseline. The corresponding experimental errors were estimated by applying linear extrapolations with gradients deviating from the best possible fits, but which were still in reasonable agreement with the experimental data. It is to be pointed out, however, that the AEs given below do not correspond to the thermochemical thresholds of the respective ion dissociations, but only provide a qualitative frame for the energy demands of the various fragmentations.[26,27]

Some additional experiments were performed on a TSQ Classic mass spectrometer equipped with an ESI source. The instrument bears a QOQ configuration (O stands for octopole) and thereby allows the performance of a variety of MS/MS experiments.[28] The results obtained with both instruments are in very good agreement. In this paper, we refer to the data set obtained at the VG BioQ unless noted otherwise.

The gas-phase infrared (IR) spectra of mass-selected ions were recorded by using a Bruker Esquire 3000 ion trap mounted to an infrared laser.[29] The infrared light was generated by a free electron laser at CLIO (Centre Laser Infrarouge Orsay, France). CLIO was operated in the 40–45 MeV range, and it gave laser beams covering a spectrum roughly ranging from 900–1800 cm^{-1}. The ions of interest were generated by ESI, mass-selected, and stored in the ion trap. The ion fragmentation was induced by 1–4 laser pulses admitted to the ion trap, and the dependence of the fragmentation intensities on the wavelength of the IR light then led to infrared multiphoton dissociation (IRMPD) spectra.

Quantum chemical calculations were performed to establish structures and relative energies of relevant isomers for the species under study and to allow a detailed assignment of the modes in their vibrational spectra. Energies and optimized geometries were obtained at the B3LYP level of density functional theory (DFT) employing the TZVP basis sets as implemented in the Gaussian 03 package.[30–38] Harmonic vibrational frequencies and zero point vibrational energies (ZPVEs) were computed at the same level of theory from analytically derived Hessian matrices by standard routines implemented in the Gaussian program. Relative energies reported refer to enthalpy differences ΔH at 0 K, which were obtained by summing total energies and (unscaled) ZPVE contributions. Comparative studies of theoretically derived and experimentally measured heats of formation of various molecules show that the accuracy of the B3LYP functional is usually better than ±0.2 eV when used in combination with basis sets of triple-ζ quality.[39,40] To validate the DFT description for the energetic ordering of isomers additional post-Hartree–Fock calculations at the CCSD(T) level were performed on all $[Cu(PhOH)]^+$ and $[Cu(PhOH)]^+$ isomers, based on the DFT-optimized structures. The cc-pVDZ and cc-pVTZ basis sets for C, O, and H atoms[41] were used in combination with the pseudopotential-based correlation consistent cc-pVDZ-PP and cc-pVTZ-PP basis sets of Peterson and Puzzarini[42] and the relativistic small-core pseudopotential developed by Figgen et al.[43] for Cu. These calculations were performed using the program Molpro.[44]

Results and Discussion

Electrospray ionization of an aqueous solution of copper nitrate and phenol provides the complex $[Cu(PhOH)(PhO)]^+$ with the expected isotope pattern (Ph = phenyl). The ionization conditions were kept either relatively mild in order to generate the complexes with two phenol-based ligands in the ESI source, or the source was operated under harsher conditions at which the monoligated complexes $[Cu(PhO)]^+$ and $[Cu(PhOH)]^+$ are generated preferentially.[27a,45,46] Accordingly, both types of complexes are chosen as model systems for CID experiments, IRMPD spectra, and theoretical investigations.

We first established the structures and relative stabilities of the isomers that arise from coordination of the copper ion either to the non-bonding electrons of the oxygen atom or to the π-electron system of the aromatic rings by means of DFT computations. The results for phenol (Figure 1)

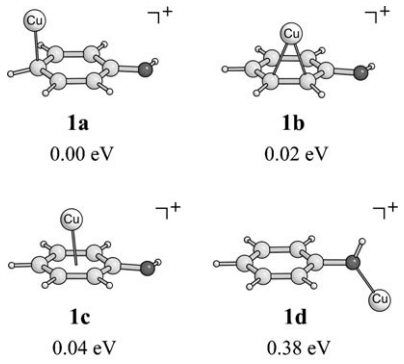

Figure 1. Structures of $[Cu(PhOH)]^+$ obtained by B3LYP/TZVP and energies (in eV) relative to the most stable species **1a**.

clearly show that the copper ion preferentially binds to the π-electron system of the aromatic ring rather than to the oxygen lone pairs. The most stable structure **1a** corresponds to a η^1-coordination mode with copper bound to the *para*-carbon atom. The η^2- and η^6-coordination modes in **1b** and **1c** are slightly less stable, but all three isomers lie very close in energy.[47–50] It is therefore reasonable to expect that the energy barriers between these isomers are also small.[51] Such a situation results in a dynamic equilibrium between all π-bound structures, which can be termed as a "copper ring-walk" in analogy to the well-known "hydrogen ring-walk" reported for protonated aromatic compounds.[52–55] In contrast, interaction of the copper ion with the oxygen atom of phenol leads to the least stable structure (**1d**) of the [Cu-

$(PhOH)]^+$ complexes studied here. We further considered a potential rearrangement of the hydrogen atom, from the oxygen atom to the ring, and we identified the corresponding complexes derived from 2,4-cyclohexanedienone and 2,5-cyclohexanedienone with copper bound to the oxygen atom (not shown), which are 0.32 and 0.22 eV, respectively, higher in energy relative to **1a**. Thus, all isomers with copper bound to the oxygen atom lie considerably higher in energy than the π-bound structures.

Preferential coordination of copper at carbon is rather unexpected considering the wealth of literature on metal binding to phenol-based ligands (such as tyrosine) in the biological context, in which solely O coordination of metal ions is suggested. However, our present results for the structures and energetic ordering of $[Cu(PhOH)]^+$ isomers are in full agreement with the previous computational investigations of Corral et al.[51] and Sodupe and co-workers.[56] Furthermore, π coordination of naked Cu^+ is perfectly consistent with well-established concepts for metal-ion coordination,[49,57–60] and indeed, crystallographic evidence for η^1-, η^2-, and η^6-coordination of Cu^I to arenes[61–65] exists, including examples for preferential π- rather than O-binding of Cu^I to *p*-benzoquinones.[66,67]

As the second part of our model system, we investigated the $[Cu(PhO)]^+$ fragment. This species could formally be seen as a Cu^{II} complex with a phenolate ligand or, alternatively, as a complex of Cu^I with a phenoxy radical (Scheme 2). In fact, our results consistently show that the latter description is correct, at least under gas-phase conditions: spin density distributions computed for all isomers clearly indicate that the unpaired electron is almost exclusively distributed over the atoms of the PhO ligand, with only minor contributions on the copper ion (cf. Figure 2, which exemplarily shows the spin density computed for the most stable isomer **2a**).

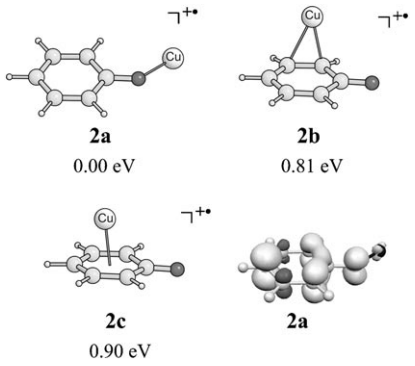

Figure 2. Structures of $[Cu(PhO)]^+$ calculated by B3LYP/TZVP and energies (in eV) relative to the most stable species **2a**; the bottom right graphic exemplarily shows the computed spin density of **2a** (α-spin: light gray, β-spin: dark gray, isosurface at 0.005 a.u.), corresponding figures result for **2b** and **2c** (not shown).

For the $[Cu(PhO)]^+$ system, we identified three isomers with different copper binding modes (Figure 2). While these structures are all in accordance with those identified for $[Cu(PhOH)]^+$, we were unable to locate a stable η^1-minimum structure corresponding to **1a**, the most stable $[Cu(PhOH)]^+$ isomer. All attempts to optimize such a minimum led to **2b** or **2c** instead. Also, in striking contrast to the results obtained for the phenol system, copper coordination to the oxygen atom (**2a**) is energetically significantly more favored than coordination to the π-system of the aromatic ring in the $[Cu(PhO)]^+$ complex: the η^2-isomer **2b** and the η^6-complex **2c** lie 0.81 and 0.90 eV, respectively, higher in energy than **2a**.

We validated the DFT results for the energetic ordering of isomers of **1** and **2** by additional CCSD(T) single-point calculations employing the cc-pVDZ(PP) and cc-pVTZ(PP) basis sets. The results in Table 1 reveal some differences between DFT and coupled cluster theory, but the qualitative DFT picture is nicely confirmed by the CCSD(T) calculations: π coordination is favored over O coordination for isomers of **1**, and vice versa for isomers of **2**.

Table 1. Energies of isomers [ΔH at 0 K in eV] relative to the most stable species for **1** and **2**. CCSD(T) results are based on B3LYP/TZVP structures and ZPVE contributions. Coupled cluster results were extrapolated to the basis set limit (index xtra) according to the linear Ansatz of Halkier et al.[76]

	1a	**1b**	**1c**	**1d**	**2a**	**2b**	**2c**
B3LYP/TZVP	0.00	0.02	0.04	0.38	0.00	0.81	0.90
CCSD(T)/cc-pVDZ(PP)	0.16	0.14	0.00	0.48	0.00	0.79	0.75
CCSD(T)/cc-pVTZ(PP)	0.14	0.11	0.00	0.56	0.00	0.74	0.74
CCSD(T)/xtra	0.13	0.10	0.00	0.56	0.00	0.72	0.75

Minor differences are observed for the energetic ordering of π-bound isomers. Contrary to the DFT results, the η^6-coordination mode in **1c** is favored over the η^1- and η^2-coordination present in **1a** and **1b** at the CCSD(T) level. Similarly, η^6-coordination is favored over η^2-coordination for the corresponding $[Cu(PhO)]^+$ isomers **2c** and **2b**. The energy differences between the π-bound isomers **1a–c** are somewhat more pronounced at the CCSD(T) level compared to the DFT results. However, since the coupled cluster calculations are based on DFT structures, we consider the observed differences not sufficiently significant to unambiguously assign the most favored coordination modes. Such discrepancies have been observed before,[68] and more definite answers would require geometry optimizations at the CCSD(T) level, but this is outside our scope at present due to the enormous numerical effort required. In any case, the CCSD(T) results also indicate a flexible coordination of copper ions to the π-face of the phenol ligand, so that the dynamical picture of a "copper ring-walk" is probably more appropriate than any static assignment of the most favorable π coordination mode. We are thus confident that our computed energetic ordering of isomers is sufficiently accurate at the DFT level to support our conclusions in the following.

Based on the results for the $[Cu(PhOH)]^+$ and $[Cu(PhO)]^+$ fragments, all conceivable coordination modes for the copper/phenoxy/phenol complex ($[Cu(PhOH)(PhO)]^+$) were considered, and four stable isomers were identified (Figure 3). The most stable complex **3a** involves a Cu–O

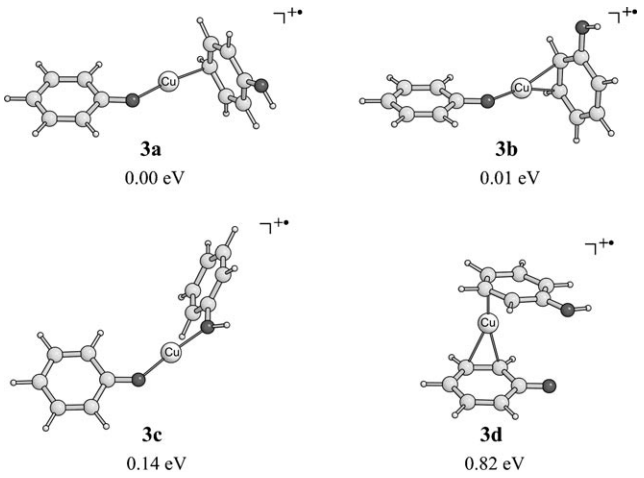

Figure 3. Structures of $[Cu(PhOH)(PhO)]^+$ calculated by B3LYP/TZVP and energies (in eV) relative to the most stable species **3a**.

bonding motif between copper and the phenoxy group and a η^1-coordination of copper to the *para* position of the ring. Thus, the most stable arrangement for the bisligated complex $[Cu(PhOH)(PhO)]^+$ involves the two most favorable binding modes identified for the monoligated species $[Cu(PhOH)]^+$ and $[Cu(PhO)]^+$. Isomer **3b**, which involves η^2-coordination in the Cu/PhOH subunit, is almost equally stable, which implies a similar structural flexibility as already suggested for the carbon-bound isomers of **1**. Interestingly, isomer **3c**, with the copper ion bound to the oxygen atoms of both ligands, is only 0.14 eV higher in energy than **3a**, whereas for **1a** and **1c** the difference between C and O coordination is 0.38 eV in favor of the former. This result suggests that the coordination of another ligand to copper diminishes the energy difference between various binding modes in the Cu(PhOH) unit. On the other hand, complex **3d** with the less favorable π coordination of copper to the phenoxy radical lies 0.82 eV above **3a**, which is nearly the same energy difference between C and O coordination as found in **2**, hence the binding mode in the Cu(PhO) unit is only negligibly influenced by the additional neutral ligand. As for **2**, the computed spin densities of isomers of **3** (not shown) reveal that the unpaired electron density almost exclusively resides on the PhO moiety, with very minor contributions on the copper ion. Hence, also in **3** the PhO ligand is correctly considered to be a phenoxy radical rather than a phenolate ligand.

In summary, binding of a phenoxy ligand to copper is found to be mediated solely by the negatively charged oxygen atom. The π coordination is energetically disfavored and this property remains unaltered in the presence of the additional phenol ligand. The strong preference for C over O coordination of Cu bound to phenol in the $[Cu(PhOH)]^+$ fragment is, in turn, reduced upon coordination of phenoxy as a second ligand. Hence, interaction of $[Cu(PhO)]^+$ with neutral phenol leads to a variety of $[Cu(PhOH)(PhO)]^+$ isomers lying very close in energy, with a large structural flexibility in the Cu···PhOH coordination. The energetically most favored arrangements arise from coordination with the carbon atoms of phenol, but binding with the oxygen atom of phenol is likely to contribute to the structural pool.

In this context we note that O coordination of copper to phenol, phenoxy, or phenolate is generally suggested as the dominant structural motif in the active centers of copper-containing enzymes, rather than binding to the π system of the aromatic ring.[20] However, our present results imply that, in the case of neutral phenol, cation–π interactions might play a more important role than anticipated previously in the discussion of copper active site structures. In this context we note that the important role of cation–π interactions has also been highlighted for the binding of main-group metals with tyrosine and other aromatic compounds.[57] The higher coordination numbers of copper ions in relevant biological environments would most likely result in a different picture, but at this point we would like to emphasize that π coordination of phenol ligands should be seen as additional flexibility of the ligand sphere at the active sites to fill vacant coordination sites around the central copper ion that arise upon substrate liberation in the course of a catalytic cycle. We suggest this view as a conceptual alternative for the usual picture, which involves intermediate coordination of exchangeable solvent molecules like water.[20] Thus, for example for GO, which has a low substrate binding affinity,[69] the stabilization of the resting states might be achieved by a simple change in the coordination mode of the tyrosine ligands rather than by the involvement of the external solvent molecules, which should be entropically disfavored. This intriguing aspect will form the subject of future investigations.

The elucidation of the structure(s) of $[Cu(PhOH)(PhO)]^+$ is further complemented by the measurement of its infrared multiphoton dissociation (IRMPD) spectrum. The structure of the investigated complex can be assessed based on the comparison of its experimental spectrum and the calculated IR spectra for the most stable isomers (Figure 4). The experimental spectrum contains five main peaks at 1176, 1285, 1345, 1512, and 1588 cm^{-1} (black lines in Figure 4). The best agreement between the experimental and theoretical spectra can be found for isomer **3b** with the relative shifts of the peak positions less than 10 cm^{-1} (Figure 4, middle). The calculated IR spectrum of isomer **3a** is also in relatively good agreement with the experimental findings, with the largest deviation for the experimental band at 1285 cm^{-1}, for which the calculated peak is blue-shifted by 21 cm^{-1}. However, both calculated spectra (for **3a** and **3b**) show a discrepancy concerning the intensities of the peaks at 1512 and 1588 cm^{-1}, which are inversed in intensity in comparison

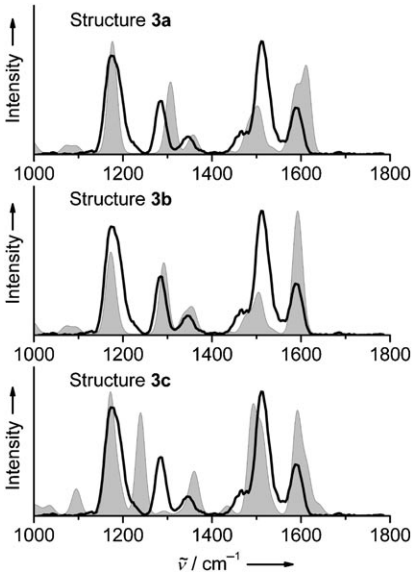

Figure 4. IRMPD spectra of $[Cu(PhOH)(PhO)]^+$ (black line) compared with the B3LYP/TZVP calculated spectra (gray area, with Gaussian broadening of all signals by 20 cm^{-1}) of the structural isomers **3a** (top), **3b** (middle), and **3c** (bottom).

with experiment. This difference is considered less significant, because the intensities obtained in IRMPD spectra do not necessarily coincide with those of a classical infrared spectrum.[70–72]

The match between the spectrum of the third isomer **3c** and the experimental one is much less satisfying. The main discrepancy again concerns the experimental peak at 1285 cm^{-1}, which is not reproduced by the calculations. The computed spectrum, on the other hand, contains an intense peak at 1239 cm^{-1}, which is not present in the experimental spectrum. A more detailed inspection of the experimental spectrum reveals that the peak at 1176 cm^{-1} has a small shoulder at about 1225 cm^{-1}. Modeling of this composite peak by three Gaussian functions suggests that this shoulder might be due to the peculiar peak at 1239 cm^{-1} in the spectrum of **3c**. Thus, this feature in the spectrum could be evidence for a small population of the isomer **3c** along with the dominant contributions of isomers **3a** and **3b**.

Based on comparison with the calculated spectra of **3a** and **3b**, the experimental bands can be assigned in the following manner: the peak at 1176 cm^{-1} corresponds to the C–O–H bending mode of the phenol ligand; the peak at 1285 cm^{-1} reflects the C–O stretching vibration of the phenol ligand; the smaller peak at 1345 cm^{-1} is assigned to the C–H bending modes of PhOH; the peak at 1512 cm^{-1} is also due to C–H bending modes of PhOH with a contribution from the C–O stretching mode of the phenoxy ligand. The latter mode gains intensity when the copper ion is coordinated to both oxygen atoms, as seen in Figure 4 (bottom). Finally, the peak at 1588 cm^{-1} corresponds to the C–C stretching vibrations in both ligands. For a more detailed discussion of the computed spectra see the Appendix.

We note in passing that the calculated spectra of copper complexes with 2,4-cyclohexanedienone and 2,5-cyclohexanedienone are substantially different from the experimental spectra. In particular, neither of the theoretical spectra exhibits any peak around 1176 cm^{-1}, in agreement to the assignment of this particular peak to the C–O–H bending mode, which cannot be present in the dienone complexes.

Unfortunately, attempts to record the IRMPD spectra for the monoligated complexes $[Cu(PhO)]^+$ and $[Cu(PhOH)]^+$ were not successful. The complex $[Cu(PhOH)]^+$ was not generated in a sufficient amount in the ESI source of the IRMPD instrument, whereas the ion yield of $[Cu(PhO)]^+$ was sufficient, but the ion underwent a rapid association with water present as a background gas in the ion-trap mass spectrometer used in these experiments.

Bond energies of $[Cu(PhOH)(PhO)]^+$: The binding energies between copper and the phenol or phenoxy ligand are derived from the analysis of collision-induced dissociation (CID) mass spectra at variable collision energies. CID of $[Cu(PhOH)(PhO)]^+$ leads to $[Cu(PhO)]^+$ and $[Cu(PhOH)]^+$ as the two major products. The dependences of the fragment abundances on the collision energy in the CID experiments allow the evaluation of the respective appearance energies (AEs) for the various dissociations (Figure 5).[26,27] The appearance energy for the loss of the

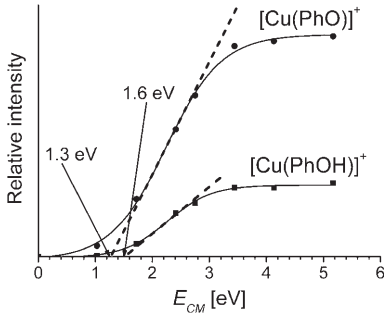

Figure 5. Example of a fit of relative intensities of the ionic fragments $[Cu(PhOH)]^+$ and $[Cu(PhO)]^+$ upon CID of mass-selected $[Cu(PhOH)(PhO)]^+$ with xenon as collision gas.

phenoxy radical from $[Cu(PhOH)(PhO)]^+$ accordingly amounts to 1.6 ± 0.2 eV and that for the loss of phenol to 1.3 ± 0.2 eV. At first sight, the small difference between the appearance energies of the ligand losses from $[Cu(PhOH)(PhO)]^+$ might be surprising, because two apparently different, coordinative and covalent, bonds are cleaved. However, the calculations suggest that the bonding of Cu^{II} with the phenolate anion is associated with electron transfer; this effectively leads to Cu^{I} and the phenoxy ligand, and therefore the bonding of both the neutral phenol and the phenoxy ligand to the copper ion is of coordinative nature. The similarity of the binding energies appears as a particular highlight of the Cu^{I}/Cu^{II} couple in conjunction with phenolate as a redox-active ligand.

These experimental results are fully consistent with the calculated values. The calculated energy necessary for the dissociation of $[Cu(PhOH)(PhO)]^+$ to $[Cu(PhOH)]^+$ and $PhO^\bullet$ is 2.1 eV, and that for the dissociation to $[Cu(PhO)]^+$ and PhOH is 1.8 eV. The calculated bond energies are somewhat larger than those determined experimentally, which can mostly be attributed to shortcomings of the appearance energy measurements, which underestimate the true thermochemical threshold.[27a,c] Accordingly, we will preferentially consider the calculated energies in the following discussion.

The influence of the counterions from the copper salts on the complex formation is considered too, because it might have a non-negligible effect on the internal energy of the cationic species generated. If there is such an effect, then it is most probably a consequence of how the complex is generated in the ESI source, which in turn may affect the relative abundances of the product ions produced in the dissociation of $[Cu(PhOH)(PhO)]^+$ generated from an aqueous solution of phenol and $Cu(NO_3)_2$, $CuCl_2$, and $CuBr_2$. The data obtained (Table 2) demonstrate that the energies for binding

Table 2. Appearance energies [in eV] for the losses of phenol and phenoxy ligands in $[Cu(PhOH)(PhO)]^+$ complexes as determined from CID experiments. The parent complex was generated from aqueous solutions of phenol and $Cu(NO_3)_2$, $CuCl_2$, and $CuBr_2$. The last row gives ΔAE [eV].

	NO_3	Cl	Br	Average
AE(-PhOH)	1.3	1.4	1.4	1.4 ± 0.2
AE(-PhO)	1.6	1.7	1.5	1.6 ± 0.2
ΔAE	0.3	0.3	0.1	0.2 ± 0.2

of the phenol and the phenoxy ligand to copper in $[Cu(PhOH)(PhO)]^+$ agree within the experimental error and do not depend on the nature of the copper salt used for the generation of the parent complex. The average binding energy for phenol is 1.4 ± 0.2 eV and that for a phenoxy radical is 1.6 ± 0.2 eV.

Bond energies of $[Cu(PhO)]^+$: The same procedure is used for the determination of the bond energy of the phenoxy ligand in $[Cu(PhO)]^+$. The major channel in the CID spectrum of $[Cu(PhO)]^+$ corresponds to the loss of a phenoxy radical to afford bare Cu^+. In addition, minor loss of a fragment with $m/z=28$ is observed, which is probably due to $[Cu(C_5H_5)]^+$ and is assigned to the expulsion of CO from the phenoxy ligand.[28] Although the elimination of a phenoxy radical might appear in competition with the sequential expulsions of CO and C_5H_5, the investigation of the fragmentation behavior of $[Cu(PhO)]^+$ in dependence of collision energy suggests the opposite: the onset of the $PhO^\bullet$ is very steep in comparison with that of the CO loss, and therefore a direct Cu–O bond cleavage, rather than consecutive eliminations of CO and C_5H_5, is expected. The appearance energy for the loss of a phenoxy radical from mass-selected $[Cu(PhO)]^+$ is determined as 2.2 ± 0.2 eV. In comparison, the B3LYP calculations again predict a slightly higher dissociation energy of 2.6 eV (see above).

As expected, the binding of the phenoxy radical to the naked copper ion is stronger than that of $PhO^\bullet$ in the bisligated complex $[Cu(PhOH)(PhO)]^+$. In turn, this implies that the coordination of a neutral ligand to the copper ion weakens the interaction between the copper center and the phenoxy ligand. Based on calculations, a similar trend emerges in that the binding energy between the copper atom and the phenoxy radical is estimated as 2.6 eV for $[Cu(PhO)]^+$ and 2.1 eV for $[Cu(PhOH)(PhO)]^+$. The relative decrease of the binding energy hence amounts to 0.5 eV, and is in reasonable agreement with the experimental difference of the AEs (0.8 ± 0.3 eV). Scheme 3 shows the relationships of the relevant bond energies for both major dissociation channels of $[Cu(PhOH)(PhO)]^+$ and a comparison with the bond energies of the products of dissociation.

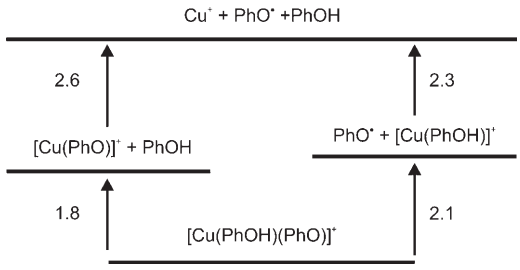

Scheme 3. Energy diagram for the complexes $[Cu(PhOH)(PhO)]^+$, $[Cu(PhO)]^+$, and $[Cu(PhOH)]^+$; all values refer to the B3LYP/TZVP calculations and are given in eV.

Conclusion

The investigation of the intrinsic properties of the $[Cu(PhOH)(PhO)]^+$ complex reveals several new findings. The computational study of the structure of the monoligated complex $[Cu(PhO)]^+$ demonstrates that copper is bound to the oxygen atom of the phenoxy ligand. On the other hand, for the $[Cu(PhOH)]^+$ complex it is shown that copper preferentially binds to the aromatic ring of phenol with bonding to the carbon atom in the *para* position being the most stable isomer. These preferences are also reflected in the bisligated complex $[Cu(PhOH)(PhO)]^+$. The theoretical results are confirmed by a pleasing agreement between the calculated IR spectra of the most stable isomers of $[Cu(PhOH)(PhO)]^+$ and the experimental IRMPD spectrum. Based on our results we suggest π coordination of Cu^+ to phenol groups as an additional flexibility of the ligand sphere at copper protein active sites.

The binding energies between copper and the ligands in $[Cu(PhO)]^+$ and $[Cu(PhOH)(PhO)]^+$ are also estimated. In the monoligated complex $[Cu(PhO)]^+$, the energy necessary for cleavage of the bond between Cu^I and the phenoxy radical amounts to 2.6 eV. The coordination of a neutral ligand to $[Cu(PhO)]^+$ results in a weakening of the bond between copper and the phenoxy ligand. The dissociation of [Cu-

$(PhOH)(PhO)]^+$ involves competitive eliminations of phenol and the phenoxy radical. The elimination of $PhO^{\bullet}$ is associated with an energy demand of 2.1 eV and that of PhOH requires 1.8 eV.

Appendix

To establish the accuracy that can be expected from the B3LYP/TZVP level of theory for the computation of vibrational frequencies for the present set of systems we studied the vibrational spectra of phenol and the phenoxy radical in some detail. Table 3 shows a comparison of the computed harmonic frequencies with recent Fourier transform infrared spectra measurements in CCl_4 for phenol in the region between 1000 and 2000 cm^{-1}.[73] While we did not perform an in-depth analysis of normal modes we note a pleasing agreement between qualitative normal mode characterizations from visual inspection of the vibrations with the detailed assignments given in reference [73]. Notwithstanding the fact that various phenol normal modes are complicated mixtures of several contributing internal coordinates we present a gross characterization of key normal modes relevant in the present context in Figure 6. Table 4 shows a comparison of recent experimental results of Spanget-Larsen et al.[74] and computed results for the phenoxy radical.

Table 3. Experimental (first column) and computed harmonic (second column) vibrational frequencies, and computed intensities of phenol in the region between 1000 and 2000 cm^{-1}.

ω [cm^{-1}]	ν [cm^{-1}]	I [km mol^{-1}]	f[a]	ω[b] [cm^{-1}]
999	1018	3.1	0.9813	997
1024	1047	5.2	0.9780	1025
1069	1097	15.4	0.9745	1074
1151	1182	54.6	0.9738	1157
1167	1193	88.3	0.9782	1168
1179	1197	18.3	0.9850	1172
1257	1280	82.1	0.9820	1253
1330	1348	8.1	0.9866	1320
1341	1374	24.9	0.9760	1345
1469	1506	24.2	0.9754	1474
1499	1533	55.5	0.9778	1501
1598	1636	42.4	0.9768	1598
1606	1648	40.8	0.9745	1610

[a] f = scaling factor. [b] Computed vibrational frequencies scaled by a uniform factor of 0.979, obtained as the arithmetic mean of individual scaling factors *f*.

Table 4. Experimental (first column) and computed harmonic (second column) vibrational frequencies of the phenoxy radical in the region between 1000 and 2000 cm^{-1}.

ω [cm^{-1}]	ν [cm^{-1}]	I [km mol^{-1}]	f[a]	ω[b] [cm^{-1}]
1038	1012	0.2	1.0258	1002
1072	1094	9.6	0.9798	1083
1140	1171	1.6	0.9735	1159
1167	1171	0.3	0.9965	1159
1266	1277	7.4	0.9911	1265
1318	1341	5.6	0.9828	1328
1397	1419	0.8	0.9844	1405
1441	1448	3.8	0.9952	1433
1481	1479	24.4	1.0014	1464
1515	1549	4.2	0.9782	1533
1550	1588	37.9	0.9758	1572

[a] f = scaling factor. [b] Computed vibrational frequencies scaled by a uniform factor of 0.990, obtained as the arithmetic mean of individual scaling factors *f*.

The data presented in Table 3 demonstrates that the deviation between experimental and computed frequencies for phenol can be reduced substantially by empirical scaling with a uniform factor of 0.979, which is obtained as the arithmetic mean of the individual scaling factors. The same procedure applied to the phenoxy results (Table 4) yields a different scaling factor of 0.990. Consideration of all vibrations for phenol and phenoxy results in a factor of 0.984, which is remarkably close to the scaling factor of 0.983 derived by Michalska et al. for the phenol vibrations.[73] However, the characteristic (i.e., most intensive) frequencies of both species do not profit consistently from empirical scaling. This is consistent with findings of Pulay and co-workers, who showed that individual scaling of force constants based on normal coordinate analyses is much more appropriate for related systems.[75] We thus refrained from any uniform scaling of vibrational modes and we based our discussion above solely on unscaled computed harmonic vibrational frequencies.

A characterization of the vibrational modes for species **3a**–**c** is shown in Figure 7. In the computed vibrational spectrum of parent phenol we find the C–O stretching frequency at 1280 cm^{-1}. Upon coordination of Cu^{I} this band is shifted to 1338 cm^{-1} (**1a**), 1305 cm^{-1} (**1b**), and 1151 cm^{-1} (**1d**). In **1c** the assignment of this mode is complicated due to strong mixing with various C–C stretching modes. Comparison with the results for the C–O stretch in **3** (**3a**: 1320 cm^{-1}, **3b**: 1304 cm^{-1}, **3c**: 1183 cm^{-1}) reveals rather similar shifts.

The computed vibrational spectrum of the isolated phenoxy radical shows two particularly intensive bands in the region between 1000 and 2000 cm^{-1}. The first peak at 1588 cm^{-1} corresponds to a C=C stretching mode and the second band at 1479 cm^{-1} corresponds to the C–O stretching motion, in good agreement with the B3LYP/cc-pVTZ (1589 and 1482 cm^{-1}, respectively) and experimental argon matrix results (1550 and 1481 cm^{-1}, respectively) of Spanget–Larsen et al.[74] In **2a** the C–C stretching band is blue-shifted to 1614 cm^{-1}, while we find two bands with significant C–O stretching contributions at 1511 and 1418 cm^{-1}.

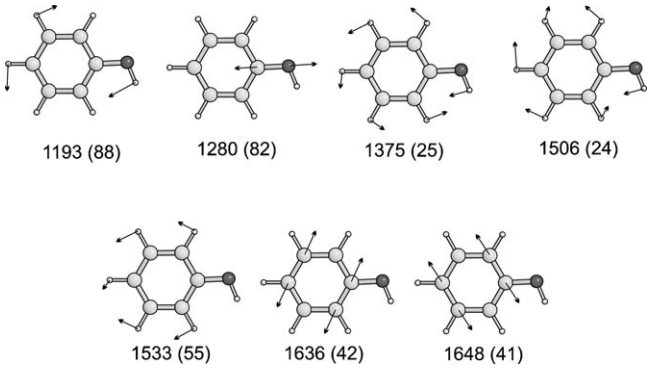

Figure 6. Qualitative characterization of selected vibrational modes computed for phenol (harmonic frequencies in cm^{-1}, relative intensities in km mol^{-1} are given in parentheses).

Acknowledgement

This work was supported by the Grant Agency of the Academy of Sciences of the Czech Republic (KJB400550704), the Ministry of Education of the Czech Republic (MSM0021620857), the Academy of Sciences of the Czech Republic (Z40550506), the Deutsche Forschungsgemeinschaft, Fonds der Chemischen Industrie, and the European Commission (EPITOPES, Project No. 15637). P.M. and D.S. received a travel grant of the European Commission to the European multi-user facility CLIO. We

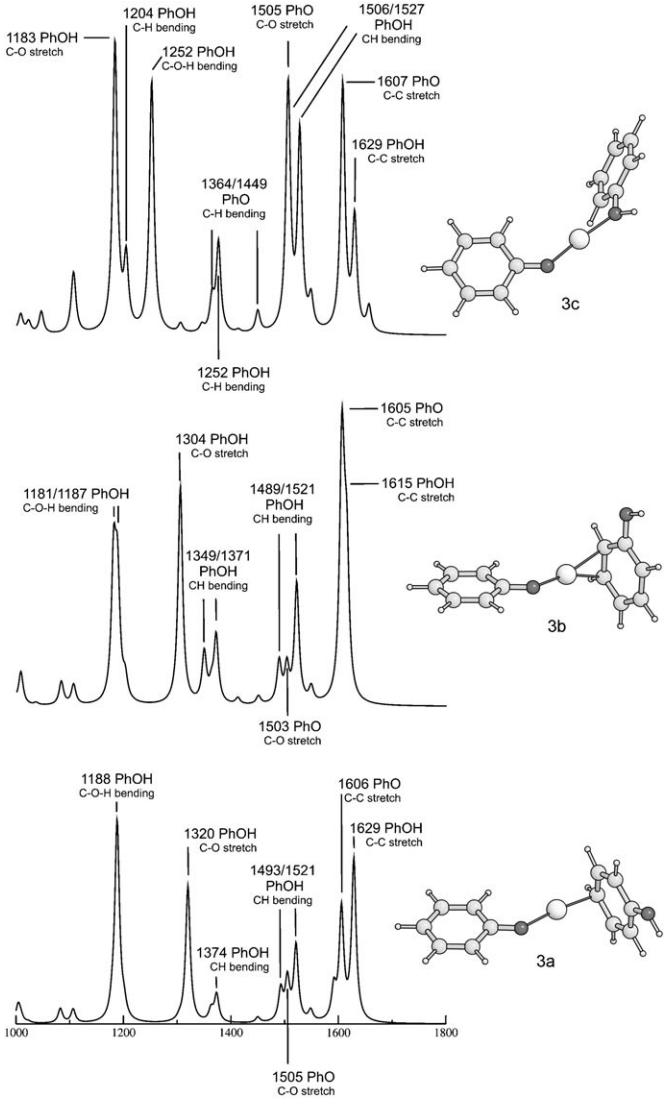

Figure 7. Calculated harmonic vibrational spectra of **3a–c** (unscaled B3LYP/TZVP results) and characterization of vibrational modes.

gratefully acknowledge support with computer time from the Frankfurt Center for Scientific Computation.

[1] W. Kaim, *Dalton Trans.* **2003**, *5*, 761–768.
[2] W. Kaim, B. Schwederski, *Bioinorganic Chemistry: Inorganic Elements in the Chemistry of Life: An Introduction and Guide* (Ed.: G. Meyer, A. Nakamura), Wiley, Chichester, **2001**, pp. 187–214.
[3] E. I. Solomon, P. Chen, M. Metz, S.-K. Lee, A. E. Palmer, *Angew. Chem.* **2001**, *113*, 4702–4724; *Angew. Chem. Int. Ed.* **2001**, *40*, 4570–4590.
[4] R. H. Holm, P. Kennepohl, E. I. Solomon, *Chem. Rev.* **1996**, *96*, 2239.
[5] W. Kaim, J. Rall, *Angew. Chem.***1996**, *108*, 47–64; *Angew. Chem. Int. Ed. Engl.* **1996**, *35*, 43–60.
[6] F. Tureček, *Mass Spectrom. Rev.* **2007**, *26*, 563–582, and references therein.
[7] L. Que Jr. , W. B. Tolman, *Angew. Chem.* **2002**, *114*, 1160–1185; *Angew. Chem. Int. Ed.* **2002**, *41*, 1114–1137.
[8] L. M. Mirica, M. Vance, D. J. Rudd, B. Hedman, K. O. Hodgson, E. I. Solomon, T. D. P. Stack, *Science* **2005**, *308*, 1890–1892.
[9] R. Malkin, B. G. Malmström, *Adv. Enzymol.* **1970**, *33*, 177–244.
[10] E. I. Solomon, M. J. Baldwin, M. D. Lowery, *Chem. Rev.* **1992**, *92*, 521–542.
[11] L. Q. Hatcher, K. D. Karlin, *J. Biol. Inorg. Chem.* **2004**, *9*, 669–683.
[12] E. I. Solomon, R. K. Szilagyi, S. DeBeer George, L. Basumallick, *Chem. Rev.* **2004**, *104*, 419–458.
[13] E. I. Solomon, R. Sarangi, J. S. Woertink, A. J. Augustine, J. Yoon, S. Ghosh, *Acc. Chem. Res.* **2007**, *40*, 581–591.
[14] C. J. Cramer, W. B. Tolman, *Acc. Chem. Res.* **2007**, *40*, 601–608.
[15] E. A. Lewis, W. B. Tolman, *Chem. Rev.* **2004**, *104*, 1047–1076.
[16] T. D. P. Stack, *Dalton Trans.* **2003**, 1881–1889.
[17] L. M. Mirica, X. Ottenwaelder, T. D. P. Stack, *Chem. Rev.* **2004**, *104*, 1013–1045.
[18] Y. Matoba, T. Kumagai, A. Yamamoto, H. Yoshitsu, M. Sugiyama, *J. Biol. Chem.* **2006**, *281*, 8981–8990.
[19] J. W. Whittaker, *Chem. Rev.* **2003**, *103*, 2347–2364.
[20] F. Thomas, G. Gellon, I. Gautier-Luneau, E. Saint-Aman, J.-L. Pierre, *Angew. Chem.* **2002**, *114*, 3173–3176; *Angew. Chem. Int. Ed.* **2002**, *41*, 3047–3050.
[21] L. Guidoni, K. Spiegel, M. Zumstein, U. Röthlisberger, *Angew. Chem.* **2004**, *116*, 3348–3351; *Angew. Chem. Int. Ed.* **2004**, *43*, 3286–3289.
[22] P. Chaudhuri, M. Hess, T. Weyhermüller, K. Wieghardt, *Angew. Chem.* **1999**, *111*, 1165–1168; *Angew. Chem. Int. Ed.* **1999**, *38*, 1095–1098.
[23] M. M. Whittaker, P. J. Kersten, D. Cullen, J. W. Whittaker, *J. Biol. Chem.* **1999**, *274*, 36226–36232.
[24] J. Roithová, D. Schröder, *Chem. Eur. J.* **2008**, *14*, 2180–2188.
[25] D. Schröder, T. Weiske, H. Schwarz, *Int. J. Mass Spectrom.* **2002**, *219*, 729–738.
[26] D. Schröder, M. Engeser, M. Brönstrup, C. Daniel, J. Spandl, H. Hartl, *Int. J. Mass Spectrom.* **2003**, *228*, 743–757.
[27] a) C. Trage, D. Schröder, H. Schwarz, *Chem. Eur. J.* **2005**, *11*, 619–627; b) P. Gruene, C. Trage, D. Schröder, H. Schwarz, *Eur. J. Inorg. Chem.* **2006**, *22*, 4546–4552; c) B. Jagoda-Cwiklik, P. Jungwirth, L. Rulisek, P. Milko, J. Roithová, J. Lemaire, P. Maitre, J. M. Ortega, D. Schröder, *ChemPhysChem* **2007**, *8*, 1629–1939.
[28] a) J. Roithová, D. Schröder, *Phys. Chem. Chem. Phys.* **2007**, *9*, 731–738; b) J. Roithová, D. Schröder, J. Míšek, I. G. Stará, I. Starý, *J. Mass Spectrom.* **2007**, *42*, 1233–1237.
[29] L. Mac Aleese, A. Simon, T. B. McMahon, J. M. Ortega, D. Scuderi, J. Lemaire, P. Maitre, *Int. J. Mass Spectrom.* **2006**, *249*, 14–20.
[30] S. H. Vosko, L. Wilk, M. Nusair, *Can. J. Phys.* **1980**, *58*, 1200–1211.
[31] C. Lee, W. Yang, R. G. Parr, *Phys. Rev. B* **1988**, *37*, 785–789.
[32] A. D. Becke, *Phys. Rev. A* **1988**, *38*, 3098–3100.
[33] A. D. Becke, *J. Chem. Phys.* **1993**, *98*, 5648–5652.
[34] J. B. Perdew, *Phys. Rev. B* **1986**, *33*, 8822–8824.
[35] P. J. Stephens, F. J. Devlin, C. F. Chabalowski, M. J. Frisch, *J. Phys. Chem.* **1994**, *98*, 11623–11627.
[36] B. Miehlich, A. Savin, H. Stoll, H. Preuss, *Chem. Phys. Lett.* **1989**, *157*, 200–206.
[37] Gaussian 03, Revision C.02, M. J. Frisch, G. W. Trucks, H. B. Schlegel, G. E. Scuseria, M. A. Robb, J. R. Cheeseman, J. A. Montgomery, Jr., T. Vreven, K. N. Kudin, J. C. Burant, J. M. Millam, S. S. Iyengar, J. Tomasi, V. Barone, B. Mennucci, M. Cossi, G. Scalmani, N. Rega, G. A. Petersson, H. Nakatsuji, M. Hada, M. Ehara, K. Toyota, R. Fukuda, J. Hasegawa, M. Ishida, T. Nakajima, Y. Honda, O. Kitao, H. Nakai, M. Klene, X. Li, J. E. Knox, H. P. Hratchian, J. B. Cross, V. Bakken, C. Adamo, J. Jaramillo, R. Gomperts, R. E. Stratmann, O. Yazyev, A. J. Austin, R. Cammi, C. Pomelli, J. W. Ochterski, P. Y. Ayala, K. Morokuma, G. A. Voth, P. Salvador, J. J. Dannenberg, V. G. Zakrzewski, S. Dapprich, A. D. Daniels, M. C. Strain, O. Farkas, D. K. Malick, A. D. Rabuck, K. Raghavachari, J. B. Foresman, J. V. Ortiz, Q. Cui, A. G. Baboul, S. Clifford, J. Cioslowski, B. B. Stefanov, G. Liu, A. Liashenko, P. Piskorz, I. Komaromi, R. L. Martin, D. J. Fox, T. Keith, M. A. Al-Laham, C. Y. Peng, A. Nanayakkara, M. Challacombe, P. M. W. Gill, B. Johnson, W. Chen, M. W. Wong, C. Gonzalez, J. A. Pople, Gaussian, Inc., Wallingford CT, **2004**.

[38] A. Schäfer, C. Huber, R. Ahlrichs, *J. Chem. Phys.* **1994**, *100*, 5829–5835.
[39] C. W. Bauschlicher, Jr., A. Ricca, H. Partridge, S. R. Langhoff in *Recent Advances in Density Functional Methods, Part II* (Ed.: D. P. Chong), World Scientific, Singapore, **1997**, pp. 165–228.
[40] W. Koch, M. C. Holthausen *A Chemist's Guide to Density Functional Theory*, Wiley-VCH, Germany, **2000**, pp. 157–163.
[41] T. H. Dunning, Jr., *J. Chem. Phys.* **1989**, *90*, 1007–1023.
[42] K. A. Peterson, C. Puzzarini, *Theor. Chem. Acc.* **2005**, *114*, 283–296.
[43] D. Figgen, G. Rauhut, M. Dolg, H. Stoll, *Chem. Phys.* **2005**, *311*, 227–244.
[44] Molpro, a package of ab initio programs designed by H.-J. Werner, P. J. Knowles, version 2006.1, R. D. Amos, A. Bernhardsson, A. Berning, P. Celani, D. L. Cooper, M. J. O. Deegan, A. J. Dobbyn, F. Eckert, C. Hampel, G. Hetzer, P. J. Knowles, T. Korona, R. Lindh, A. W. Lloyd, S. J. McNicholas, R. R. Manby, W. Meyer, M. E. Mura, A. Nicklass, P. Palmieri, R. Pitzer, G. Rauhut, M. Schütz, U. Schumann, H. Stoll, A. J. Stone, R. Tarroni, T. Torsteinsson, H.-J. Werner, **2007**.
[45] N. B. Cech, C. G. Enke, *Mass Spectrom. Rev.* **2001**, *20*, 362–387.
[46] a) N. Tsierkezos, D. Schröder, H. Schwarz, *J. Phys. Chem. A* **2003**, *107*, 9575–9581; b) C. Trage, M. Diefenbach, D. Schröder, H. Schwarz *Chem. Eur. J.* **2006**, *12*, 2454–2464.
[47] Ch. N. Yang, S. J. Klippenstein, *J. Phys. Chem. A* **1999**, *103*, 1094–1103.
[48] P. Chaquin, D. Costa, Ch. Lepetit, M. Che, *J. Phys. Chem. A* **2001**, *105*, 4541–4545.
[49] J. C. Ma, D. A. Dougherty, *Chem. Rev.* **1997**, *97*, 1303–1324.
[50] T. K. Dargel, R. H. Hertwig, W. Koch, *Mol. Phys.* **1999**, *96*, 583–591.
[51] I. Corral, O. Mó, M. Yáñez, *Int. J. Mass Spectrom.* **2006**, *255–256*, 20–27.
[52] D. Kuck, *Mass Spectrom. Rev.* **1990**, *9*, 187–233.
[53] D. Kuck, *Mass Spectrom. Rev.* **1990**, *9*, 583–630.
[54] D. Schröder, J. Loos, H. Schwarz, R. Thissen, O. Dutuit, *J. Phys. Chem. A* **2004**, *108*, 9931–9937.
[55] T. D. Jaeger, M. A. Duncan, *J. Phys. Chem. A* **2005**, *109*, 3311–3317.
[56] A. Rimola, L. Rodríguez-Santiago, M. Sodupe, *J. Phys. Chem. B* **2006**, *110*, 24189–24199.
[57] D. A. Dougherty, *Science* **1996**, *271*, 163–168.
[58] S. M. Hubig, S. V. Lindeman, J. K. Kochi, *Coord. Chem. Rev.* **2000**, *200–202*, 831–873.
[59] D. T. Moore, J. Oomens, J. R. Eyler, G. von Helden, G. Meijer, R. C. Dunbar, *J. Am. Chem. Soc.* **2005**, *127*, 7243–7254.
[60] T. Osako, Y. Tachi, M. Doe, M. Shiro, K. Ohkubo, S. Fukuzumi, S. Itoh, *Chem. Eur. J.* **2004**, *10*, 237–246.
[61] E. D. Blue, T. B. Gunnoe, J. L. Peterson, P. D. Boyle, *J. Organomet. Chem.* **2006**, *691*, 5988–5993.
[62] M. Mascal, J. Hansen, A. J. Blake, W.-S. Li, *Chem. Commun.* **1998**, 355–356.
[63] A. M. Dattelbaum, J. D. Martin, *Polyhedron* **2006**, *25*, 349–359.
[64] T. Osako, Y. Tachi, M. Taki, S. Fukuzumi, S. Itoh, *Inorg. Chem.* **2001**, *40*, 6604–6609.[]
[65] F.-B. Xu, Q.-S. Li, L.-Z. Wu, X.-B. Leng, Z.-C. Li, X.-S. Zeng, Y. L. Chow, Z.-Z. Zhang, *Organometallics* **2003**, *22*, 633–640.
[66] T. Uechi, H. Yamaguchi, I. Ueda, K. Yasukouchi, *Bull. Chem. Soc. Jpn.* **1980**, *53*, 3483–3487.
[67] B. Lenders, W. Kläui, M. Irmler, G. Meyer, *J. Chem. Soc. Dalton Trans.* **1990**, 2069–2075.
[68] C. Ruan, Z. Yang, M. T. Rodgers *Phys. Chem. Chem. Phys.* **2007**, *9*, 5902–5918.
[69] M. M. Whittaker, D. P. Ballou, J. W. Whittaker, *Biochemistry* **1998**, *37*, 8426–8436.
[70] J. Oomens, B. G. Sartakov, G. v. Helden, G. Meijer, *Int. J. Mass Spectrom.* **2006**, *254*, 1–19.
[71] D. Schröder, H. Schwarz, P. Milko, J. Roithová, *J. Phys. Chem. A* **2006**, *110*, 8346–8353.
[72] N. C. Polfer, J. Oomens, R. C. Dunbar, *Phys. Chem. Chem. Phys.* **2006**, *8*, 2744–2751.
[73] D. Michalska, W. Zierkiewicz, D. C. Bienko, W. Wojciechowski, T. Zeegers-Huyskens *J. Phys. Chem. A* **2001**, 105, 8734–8739.
[74] J. Spanget-Larsen, M. Gil, A. Gorski, D. M. Blake, J. Waluk, J. G. Radziszewski *J. Am. Chem. Soc.* **2001**, 123, 11253.
[75] a) J. Baker , A. A. Jarzecki, P. Pulay *J. Phys. Chem. A* **1998**, 102, 1412–1424; b) G. Rauhut, P. Pulay *J. Phys. Chem.* **1995**, 99, 3093–3100.
[76] A. Halkier, T. Helgaker, P. Jørgensen, W. Klopper, H. Koch, J. Olsen, A. Wilson, *Chem. Phys. Lett.* **1998**, *286*, 243–252.

Received: January 10, 2008
Published online: March 26, 2008

